International Journal of Innovative Computing, Information and Control
Volume **11**, Number **3**, June **2015**

 ISSN 1349-4198
pp. 1075–1091

CALCULATING PHASE TRANSITION WIDTHS IN PRODUCTION FLOW PROCESSES USING AN AVERAGE REGRESSION MODEL

Kenji Shirai[1] and Yoshinori Amano[2]

[1]Faculty of Information Culture
Niigata University of International and Information Studies
3-1-1, Mizukino, Nishi-ku, Niigata 950-2292, Japan
shirai@nuis.ac.jp

[2]Kyohnan Elecs Co., LTD.
8-48-2, Fukakusanishiura-cho, Fushimi-ku, Kyoto 612-0029, Japan
y_amano@kyohnan-elecs.co.jp

Received August 2014; revised December 2014

Abstract. *In our previous study, we revealed that a phase transition phenomenon can be observed in the throughput of the manufacturing processes of certain pieces of control equipment. This phase transition corresponds to the fluctuation between sub-processes in the production flow process. In this study, we calculate the phase transition width using an average regression model. Then, we devise a representation of a stable condition in order to maintain the processes with smaller volatility. Finally, we use actual production data to show that a synchronous process is superior to an asynchronous one for obtaining high throughput.*
Keywords: Average regression model, Phase transition width, Throughput, Ginzburg-Landau free energy

1. **Introduction.** We have many years of experience in studying manufacturing operations associated with control equipment for general industrial machines. In particular, we have focused on the reduction of production throughput [1, 2, 3, 4]. Business style is a complete make-to-order production system and the production process is a batch process. We take order the production if the customer's offer is acceptable. At this time, we can get a final delivery date and an amount of money.

In the previous study [5], we constructed a state in which the production density of each process corresponds to the physical propagation of heat [6]. Using this approach, we showed that a diffusion equation dominates the manufacturing process. In other words, when minimizing the potential of the production field (stochastic field), the equation, which is defined by the production density function $S_i(x,t)$ and the boundary conditions, is described using the diffusion equation with advection to move in transportation speed ρ. The boundary conditions mean a closed system in the production field. The adiabatic state in thermodynamics represents same state [5].

The fluctuation, self-similarity and on-off intermittency are occurring in non-equilibrium dissipative system of physics. We have tried in many years that a production process is almost equal to a non-equilibrium dissipative system.

In the previous study of fluctuation [8], we clarified the self-similarity of fluctuations in a supply chain system and present a size-independent mathematical model of a supply chain system using Langevin-type stochastic differential equations. We also demonstrate that for this supply chain system, when the time constant of the time correlation function possesses a uniform poisson distribution, the system exhibits f^{-1} fluctuation and when

this time constant possesses a uniform distribution, the system exhibits f^{-2} fluctuation. Furthermore, the supply chain system has a Lorentzian spectrum under the condition of fluctuations having spectral density. We proposed that profit can be increased when adopting a strategy that purposefully leads to a state of excessive production or one of excessive order entries.

Regarding with phase transition, by introducing the Ginzburg-Landau free energy, we defined a parameter corresponding to an order parameter as a factor of the phase transition in manufacturing processes. Because thermal diffusion equations can be applied as mathematical models in the manufacturing process, we consider the applicability of the "Edge of Chaos", which is used in complex systems, to the manufacturing industry and the extent to which it would do so. We believe that in the manufacturing industry, the "Edge of Chaos" is a phenomenon that is caused by the loss of synchronization between the production and production throughput. The phase transition phenomenon is observed as the process throughput while manufacturing certain control equipment. As a result, by not exceeding the average value of the rate-of-return, we proposed that it was possible to maintain uninterrupted production [9]. Furthermore, self-similarity is present in the packet-queuing congestion that occurs in a manufacturing communication network. Our overall goal is to eliminate bottlenecks in such a network [10].

We indicated that the phase transition phenomenon is observed in the process throughput of the manufacture of certain control equipment. At that time, a production density was assumed the advection diffusion equation. We verify the phase transition in the system through experiments on a flow production system. To maintain synchronization between the production and production throughput, we need to know the critical point of the phase transition. From a business perspective, it is vital to focus on not exceeding the critical point. In the manufacturing industry, the critical point indicates the rate-of-return deviation. By not exceeding the average value of the rate-of-return, it is possible to maintain uninterrupted production. The reason for this is that the Ginzburg-Landau free energy can be treated as free energy for the manufacturing quantity between manufacturing processes. In other words, it can be considered the same as the throughput between manufacturing processes [13].

On the other hand, in an actual production setting, the throughput exhibited an average regression behavior. The average regression obeys a normal logarithm-type stochastic partial differential equation and can be evaluated at the termination time. Three tests, which consisted of an asynchronous method (Testrun1), a synchronous method involving pre- and post-processing (Testrun2), and a synchronous method (Testrun3), were performed to validate this theory. The number of devices produced during each test run and the resulting production throughput were compared. The same production volumes were obtained, validating our study.

In this study, we examine the average regression behavior of the throughput in an actual production process. The variable in the average regression differential equation is the fluctuation of manufacturing workers.

We reported the existence of a phase transition in a previous study [9]. Here we determine the phase transition width value using an average regression model. The average regression model is built in the form of a production flow process with six stages (S1-S6); this represents a commercial process for the production of control equipment that is ultimately delivered to the customer. Moreover, we present a stable condition to maintain a high throughput. Then, we present a numerical result for stability in the production flow process. We show that the regression speed has a close relationship with the throughput and volatility. Our results demonstrate that a synchronous process is the best production

method, which is in keeping with previous findings [1, 2, 3, 4]. To the best of our knowledge, this is the first study on phase transition width to be applied to the manufacturing industry.

2. **Mathematical Model of the Manufacturing Process Using an Average Regression Model.** We have reported that the analysis of the rate-of-return deviation for a certain equipment manufacturer over the past ten years has revealed "power-law distribution characteristics" [7]. Because the power-law distribution is a distribution revealing the existence of a phase transition phenomenon, we expect that there exists a correlation between the rate-of-return deviation and the production system in a manner that is mediated by the power-law distribution.

Christopher G. Langton is known for his 1990 study of artificial beings [14]. He also conceptualized the idea of the "Edge of Chaos". In physical phenomena, the "Edge of Chaos" refers to a phenomenon that corresponds to the transition state that exists between fluid and solid phases. Phenomena similar to the "Edge of Chaos" occur during the period from the entry of the manufacturing order for a product to its delivery. When an order for manufacturing is received, there exists an outflow of cash due to the purchase of materials for the person receiving the order, and there is a lead time until cash is injected at the end of the manufacturing period. To increase the rate-of-return, it is important to reduce the lead time from a financial perspective. In addition, the rate-of-return is decreased if opportunities are lost and if there are excessive inventory stocks. From a practical perspective, it is necessary to synchronize the speeds of individual manufacturing operations. We consider that the synchronization of manufacturing processes will lead to the improvement of the production throughput. Here, the synchronization of manufacturing processes is one method to enable the efficient progress of each process in order to increase the throughput.

By synchronizing the processes, each process will become more time efficient. In the under-production flow in Figure 1, because the production throughput is low relative to the production output, opportunity loss occurs (for example, a state where the shipping quantity is small owing to endogenous and exogenous factors). In addition, in the over-production flow in Figure 1, because the throughput is very high relative to the production output, there will be excessive inventory. In any case, when such a probability structure exists, it is considered that a phase transition phenomenon occurs in the production field. Therefore, production management needs to be performed with this in mind. More detail is described in our previous study [9].

When considering like this, we define potential energy (free energy) in a production field as follows.

Definition 2.1. *Potential energy in production field*

$$\begin{aligned}&[\textit{Potential of production field per production density}]\\ =&[\textit{Potential for production unit}]\\ &+[\textit{Fluctuation of potential for production unit}]\end{aligned}$$

Such definition is almost equivalent to definition of the potential or free energy of a field in physics. We consider that a return is generated by temporal deviation of a potential function (free energy) attributed to a production density function. Therefore, let a cash flow function for each $t_k \in [0, T_k]$, $k = 0, 1, 2, \cdots$ be $P_k(t_p)$ (hereinafter, the subscript k is omitted).

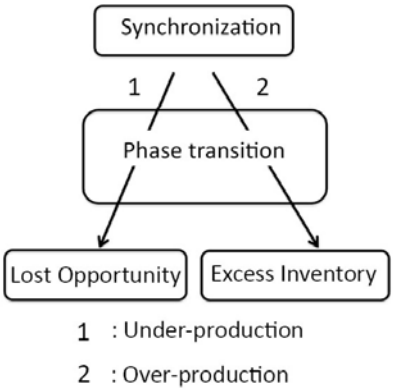

FIGURE 1. Lost opportunity (1: Under-production) and Excess inventory (2: Over-production)

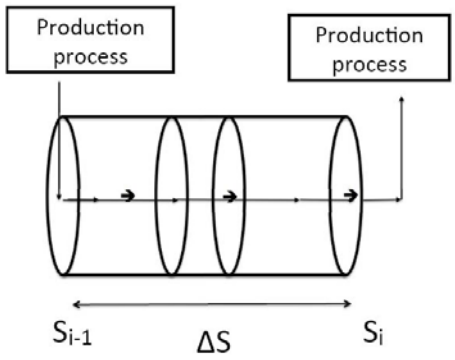

FIGURE 2. Progress difference between the two inter-process

Definition 2.2. *Definition of the traffic flow model*

$$v(t+\tau) = \Big[v(t) + \alpha\{v_{opt} - v(t)\}\tau\Big](1+z) \tag{1}$$

where, $z = f_{noise}\xi$, f_{noise} *is the noise intensity, and* ξ *is a uniform random number.*

The traffic density is $1/f_{noise}$, which is a characteristic of traffic flow theory. When f^2_{noise} increases, the average traffic density also increases under f^2_{noise}. In other words, these items are defined by a stochastic phase transition equation:

$$\begin{aligned} \frac{dh}{dt} &= a\Big[v_{opt}(\Delta S) - h\Big] + \sigma(h)Z(t) \\ dh &= a\Big[v_{opt}(\Delta S) - h\Big]dt + \sigma(h)dW(t) \end{aligned} \tag{2}$$

where $Z(t)\cdot dt = dW(t)$, $h \equiv \partial S/\partial t$ (the fluctuation speed of production density), and a is a coefficient of the regression speed.

$$dS(t) = a\Big(W_{opt}(\Delta C) - S(t)\Big)dt + \sigma dB(t), \quad C \equiv \frac{dS}{dt} \tag{3}$$

where C represents a throughput and a is a parameter [15]. The non-occurrence probability, ξ, is defined as follows [15]:

$$\begin{aligned} \frac{d\xi(t)}{dt} &= \Big(1 - \frac{D}{2M}\Big)\xi(t) + \sigma Z(t) \\ &= \mu\xi(t) + \sigma Z(t) \end{aligned} \tag{4}$$

From Equations (3) and (4), we obtain a strictly linear Langevin model equation as follows:

$$\frac{dg(t)}{dt} + mg(t) = f(t) \tag{5}$$

where, $f(t)$ is an external force (noise term).

Generally, Equation (5) is described as follows:

$$\frac{dg(t)}{dt} = f(g(t)) + \sqrt{H}Z(t) \tag{6}$$

where Equation (2) is the model equation that defines the production speed, and ΔS is the progress difference between neighboring processes.

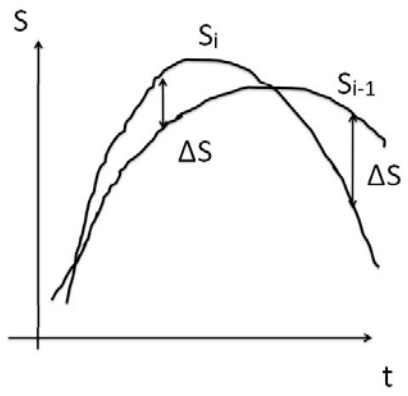

FIGURE 3. Production density (S_i and S_{i-1}) of neighboring processes

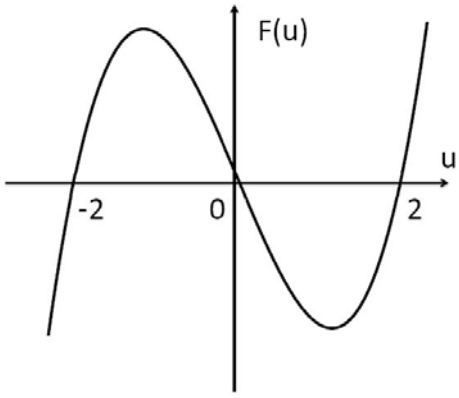

FIGURE 4. Free energy of the Ginzburg-Landau

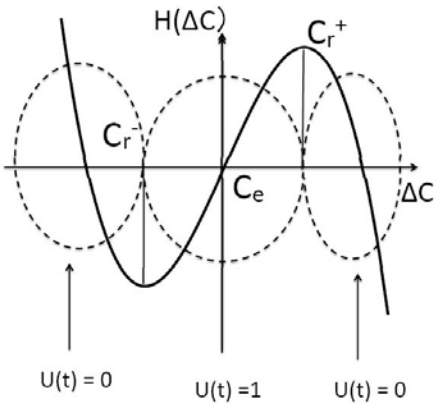

FIGURE 5. Phase transition of production process on G-L equation

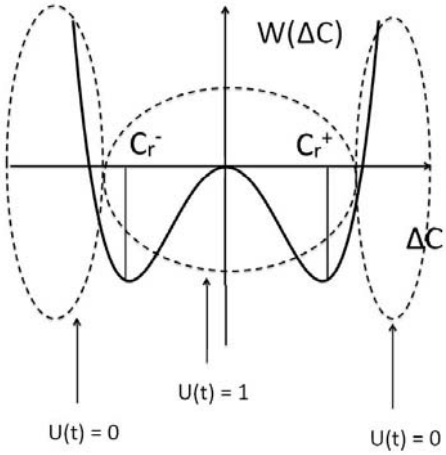

FIGURE 6. Phase transition of production process on Ginzburg-Landau free energy

3. **Ginzburg-Landau (G-L) Free Energy.** In this study, we attempt to model the synchronization state (whether it is asynchronous or synchronous in the phase transition phenomenon), which is represented in Figure 5 and Figure 6 as being surrounded by a broken line. The main variables that are used in this study are as follows:

t: time variable, $t \in [0, T]$, $\mathcal{L}^1(\bullet)$: bounded linear operator and $L^P(X)$: the space of an integral of a function f_{noise}, raised to the power of P in the space X, that is $f : \int_X |f(x)|^P dx < \infty$, where $1 < P < \infty$.

Here, we have introduced the order parameter, u, to identify the two states: asynchronous and synchronous. The order parameter u must satisfy the inequality $-\alpha < u < \alpha$ because a stable throughput has a finite range value.

The Ginzburg-Landau equation of free energy is as follows [9, 11, 16]:

$$\begin{aligned} F(u) &= \int_G \Big[\frac{r}{2}(\bigtriangledown u)^2 + W(u)\Big] dx \\ &\approx \int_G \Big[\frac{r}{2}\Big(\frac{\partial u}{\partial t}\Big)^2 + W(u)\Big] dx,\ x \in R_1 \end{aligned} \tag{7}$$

where, $(\partial u/\partial t) = -(\delta F(u)/\delta u)$. $W(u) = (1/8)u^4 - (1/4)u^2$.

$$\frac{\delta F(u)}{\delta u} = -r\frac{\partial u}{\partial t} - \frac{1}{2}(1-u^2) \tag{8}$$

$$\delta F(u) = \int_G \Big[-r\frac{\partial u}{\partial t} - \frac{1}{2}u + u^3\Big]\delta u \tag{9}$$

$$\frac{\partial u}{\partial t} = rL(u)\Delta u + \frac{1}{2}L(u)u(1-u^2) \tag{10}$$

Equation (10) is called the Ginzburg-Landau equation, and is a basic equation that describes the behavior of a phase transition. In Equation (10), we try to represent an actual situation, which is the stochastic behavior of the flow speed of production density. Then, Equation (10) is replaced as follows:

$$\frac{\partial u}{\partial t} = r\Delta u + \frac{1}{2}u(1-u^2) + u(1-u^2)\frac{\partial w}{\partial t} \tag{11}$$

where, w is a Wiener process, and represents a white noise, and we set $L(u) = 1$ for simplicity.

Here, Equation (1) is rewritten as follows:

$$\frac{\partial u}{\partial t} + v\frac{\partial u}{\partial x} = a\Big(u_{opt}(\Delta\rho) - u\Big) + f(u) \tag{12}$$

where, $\Delta\rho$ represents a deviation between processes. Generally, free energy does not increase in a closed system. Therefore, we can describe the free energy as follows [11]:

$$\frac{dF(u)}{dt} = \int_G \frac{\delta F(u)}{\delta u}\cdot\frac{\partial u}{\partial t}dx \le 0 \tag{13}$$

where, $\delta F(u)/\delta u$ represents the functional derivative.

Here, there is a need to satisfy Equation (14) to satisfy Equation (13).

$$\frac{\partial u}{\partial t} = -\frac{\delta F(u)}{\delta u} \tag{14}$$

4. **Applying TDGL to a Production Flow Process.** Here, the mathematical model is derived:

$$\begin{aligned}\frac{\partial C}{\partial t} &= \mathcal{L}(C)\\ \mathcal{L}(C) &= -v\frac{\partial}{\partial x} + D\frac{\partial^2}{\partial x^2} + a\Big[C_{opt}(\Delta\rho) - 1\Big]\end{aligned} \tag{15}$$

At the product shipment stage, Equation (15) is described:

$$\frac{dC}{dt} = a\Big[C_{opt}(\Delta C) - C\Big],\ C \equiv \frac{dS}{dt} \tag{16}$$

where, dS/dt represents a throughput.

The production manager changes the throughput rate in accordance with the deviation of the production throughput between each process.

Now, let C_e represent an inflection point. Then, the G-L equation is described:

$$\frac{\partial(\Delta C)}{\partial t} = \mathcal{L}(C)\cdot\Delta C + \frac{1}{2}(\Delta C)\Big\{1 - (\Delta C)^2\Big\} \tag{17}$$

Therefore, generally it is described:

$$F(\Delta r) = F(0) + \alpha_1(C_e)(\Delta C - C_e) + \alpha_2(C_e)(\Delta C - C_e)^2 + \alpha_3(C_e)(C - C_e)^3 + \cdots \tag{18}$$

where, $\Delta r = \Delta C - C_e$, $\alpha_1(C_e)$ and $\alpha_3(C_e)$ are as follows:

$$\alpha_1(C_e) \approx \alpha_1^{'}(C_e)\left[\frac{1}{a}\frac{\partial C_{opt}(C)}{\partial t}\Big|_{\Delta C = C_e} - \frac{1}{2}\right] \tag{19}$$

$$\alpha_3(C_e) \approx \frac{1}{3!}\left[\frac{\partial^3 C_{opt}(C)}{\partial(\Delta C)^3}\Big|_{\Delta C = C_e}\right] \tag{20}$$

where even terms are assumed to be zero and terms of third order or higher are ignored.

Here, $F(0) = 0$, and we obtain as follows:

$$F(\Delta C) = \frac{\partial C_{opt}}{\partial t}\Big|_{C_{opt}=C_e} + \left[\frac{1}{a}\frac{\partial C_{opt}}{\partial t}\Big|_{C_{opt}=C_e} - \frac{1}{2}\right](\Delta C - C_e) + \frac{1}{6}\frac{\partial^3 C_{opt}}{\partial t^3}\Big|_{C_{opt}=C_e}(\Delta C - C_e)^3 \tag{21}$$

Therefore, G-L equation is derived as follows:

$$\frac{\partial(\Delta C)}{\partial t} = a\left[C_{opt} - C_e\right] - \frac{\partial C_{opt}}{\partial t}\Big|_{C_{opt}=C_e}\left[\frac{1}{a}\frac{\partial C_{opt}}{\partial t}\Big|_{C_{opt}=C_e} - \frac{1}{2}\right](\Delta C - C_e) + \frac{1}{6}\frac{\partial^3 C_{opt}}{\partial t^3}\Big|_{C_{opt}=C_e}(\Delta C - C_e)^3 \tag{22}$$

Then, by integrating Equation (22), we obtain as follows:

$$\begin{aligned} W(\Delta C) &= \int F(\Delta C)d(\Delta C) \\ &= -\frac{1}{2}C_{opt}(C_e)\left[\frac{1}{a}\frac{\partial C_{opt}}{\partial t}\Big|_{C_{opt}=C_e} - \frac{1}{2}\right](\Delta C - C_e)^2 \\ &\quad + \frac{1}{24}\frac{\partial^3 C_{opt}}{\partial t^3}\Big|_{C_{opt}=C_e}(\Delta C - C_e)^4 \end{aligned} \tag{23}$$

Then, a part of Equation (21) is replaced as follows:

$$H(\Delta C) = -\frac{1}{2}\frac{\partial C_{opt}}{\partial t}\Big|_{C_{opt}=C_e}\left[\frac{1}{a}\frac{\partial C_{opt}}{\partial t}\Big|_{C_{opt}=C_e} - \frac{1}{2}\right](\Delta C - C_e) + \frac{1}{6}\frac{\partial^3 C_{opt}}{\partial t^3}\Big|_{C_{opt}=C_e}(\Delta C - C_e)^3 \tag{24}$$

where, $C_r^- \le C \le C_r^+$.

Here, $C_{opt}(\Delta C)$ is considered as follows [9]:

$$C_{opt}(\Delta C) = \xi\left\{-R \cdot (\Delta C) + \frac{D}{3}(\Delta C)^3\right\} \tag{25}$$

Then, the first- and third-order differentials are respectively represented:

$$C_{opt}^{'}(C)\Big|_{C_{opt}=C_e} = (-R + D \cdot C_e^2) \tag{26}$$

$$C_{opt}^{'''}C\Big|_{C_{opt}=C_e} = 2D \tag{27}$$

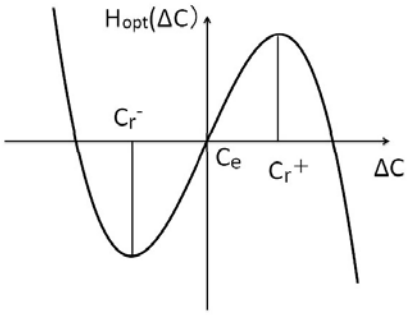

FIGURE 7. Example of G-L equation

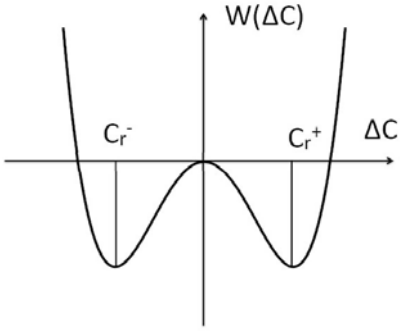

FIGURE 8. Potential function of the Ginzburg-Landau

From Equations (26) and (27), $H_{opt}(\Delta C)$ is derived as follows:

$$H(\Delta C) = \xi \left\{ -\frac{(-R + D \cdot C_e^2)}{2} \left[\frac{(-R + D \cdot C_e^2)}{a} - \frac{1}{2} \right] (\Delta C - C_e) + \frac{1}{3}(\Delta C - C_e)^3 \right\}, \quad {}^{\forall} C_r^- \leq \Delta C \leq C_r^+ \tag{28}$$

Then, The new parameter K is introduced as follows:

$$K \equiv (-R + D \cdot C_e^2) \left[\frac{(-R + D \cdot C_e^2)}{a} - \frac{1}{2} \right] \tag{29}$$

After replacing of Equation (29), we obtain as follows:

$$H_{opt}(\Delta C) = \xi \left[-K \frac{(\Delta C - C_e)}{2} + \frac{D}{3}(\Delta C - C_e)^3 \right] \tag{30}$$

Therefore, the potential function is derived as follows:

$$W(\Delta C) = \xi \left\{ -\frac{K}{4}(\Delta C - C_e)^2 + \frac{D}{12}(\Delta C - C_e)^4 \right\} \tag{31}$$

From $H(\Delta C) = 0$, the width (C) of phase transition is derived:

$$(\Delta C - C_e) \left\{ -K + \frac{D}{3}(\Delta C - C_e)^2 \right\} = 0 \tag{32}$$

Thus, as $\Delta C - C_e$ is excluded, $\Delta C - C_e$ is derived:

$$\Delta C = C_e, \text{ or } \Delta C - C_e = \sqrt{\frac{3}{D} K} \tag{33}$$

where, R and D are any parameters.

We were able to represent the width, ΔC, of the phase transition, whose exact value could not be shown in our previous paper [9].

5. Calculation of Phase Transition Width Using the Average Regression Model.

From Equation (29), when $K > 0$,

- $D \cdot C_e^2 > R$: We obtain $C_e > \sqrt{K/D}$, where K, D are any constant parameters. Then $C_e \to \infty$. Therefore, C_e is nonconformity.
- $0 < DC_e^2 < R$: We obtain $0 < C_e < \sqrt{K/D}$. C_e becomes a finite value.

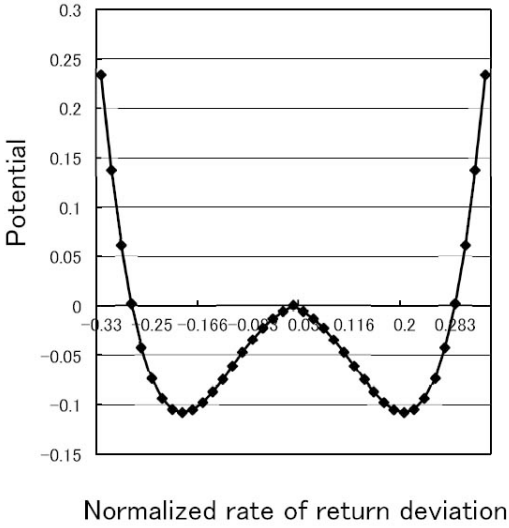

FIGURE 9. Potential function of rate of return deviation

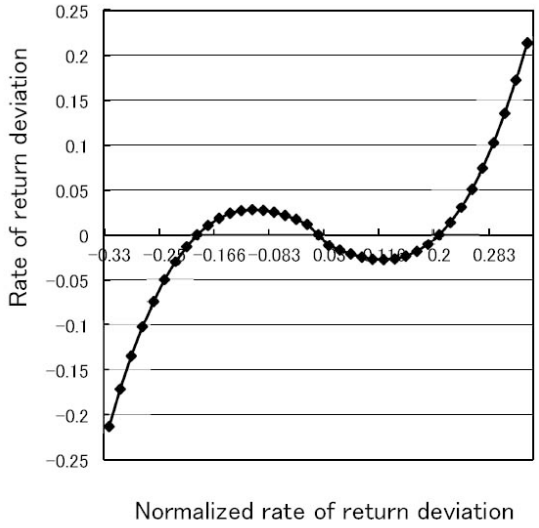

FIGURE 10. Function of rate of return deviation

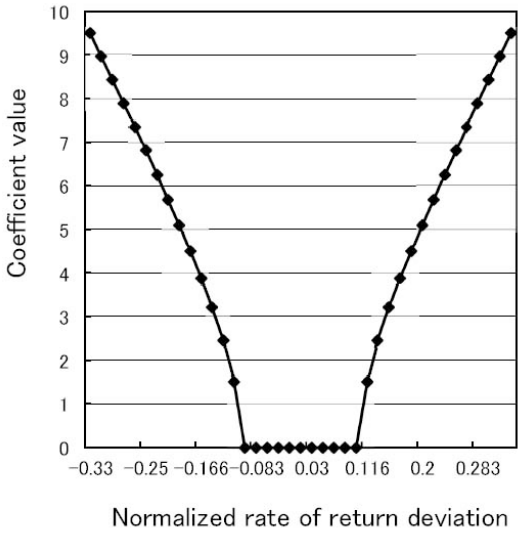

FIGURE 11. Critical rate of return deviation

Thus, we derive Equation (33), which shows that the lead time fluctuates around the inflection point.

Here, C_e is considered as the inflection point, i.e., the edge of chaos. Then, for example, $C_e \approx 0.3$ in the case of a rate of return [9].

Therefore, we obtain:

$$\Delta C = 0.3 \pm \sqrt{\frac{3K}{D}} \tag{34}$$

$$K = (-R^2 + D \cdot C_e^2) \left[\frac{(-R^2 + D \cdot C_e^2)}{a} - \frac{1}{2} \right] \tag{35}$$

Thus, $C_e^2 < D/R$, where $C_e^2 = 0.09$. Therefore, $D = 5$, $R = 0.5$, $a = 1.25$. Then, K is:

$$\begin{aligned} K &\simeq (-0.5 + 0.45)\left[\frac{-0.05}{1.25} - \frac{1}{2}\right] \\ &\approx 0.027 \end{aligned}$$

Therefore, $\Delta C = 0.3 \pm 0.127$. $0.127 < C_e < 0.427$. The parameters $a = 1.25$, $R = 0.5$, $D = 5.0$ and $C_e = 0.3$. Thus:

$$C_{opt}(\Delta C) \approx \xi\left[-0.5(\Delta C) + 1.67(\Delta C)^3\right] \tag{36}$$

In this section, using the average regression model, we derived the G-L equation and calculated the potential energy. Moreover, we represented the fluctuation around the inflection point C_e. Applying the appropriate parameters, a result which is similar to the phase transition model for the rate of return was obtained [9].

6. **Stability Analysis on Throughput Fluctuation.** The mathematical model for throughput $C(t)$ is given below:

$$\frac{dC(t)}{dt} = S_b(t) - S_{b+1}(t) \tag{37}$$

According to Equation (3),

$$\begin{aligned} \frac{dS_{b+2}(t)}{dt} &= a\Big\{W(C_{b+1}(t)) - S_{b+2}(t)\Big\} \\ \frac{dS_{b+1}(t)}{dt} &= a\Big\{W(C_b(t)) - S_{b+1}(t)\Big\} \end{aligned} \tag{38}$$

Therefore, we obtain from the average regression model [15]:

$$\frac{d^2C(t)}{dt^2} = a\left\{W(C_b(t)) - W(C_{b+1}(t)) - \frac{dC_{b+1}(t)}{dt}\right\} \tag{39}$$

where the fluctuation process of $C_b(t)$ is derived:

$$C_b(t) = C_b^0(t) + y_b(t) = \bar{C} + y_b(t) \tag{40}$$

We obtain:

$$\begin{aligned} \frac{d^2y_{b+1}(t)}{dt^2} &= \left[a\frac{\partial W(C)}{\partial C}\Big|_{C=\bar{C}}\Big\{y_b(t) - y_{b-1}(t)\Big\} - \frac{dy_{b+1}(t)}{dt}\right] \\ &= \left[aW'(\bar{C})\Big\{y_b(t) - y_{b-1}(t)\Big\} - \frac{dy_{b+1}(t)}{dt}\right] \end{aligned} \tag{41}$$

where $W'(\bar{C}) = \frac{\partial W(C)}{\partial C}\Big|_{C=\bar{C}}$.

Letting $y_b(t) = f_b e^{j\omega t}$, then, we can rewrite:

$$-\omega^2 f_{b+1} = aW'(\bar{C})\Big[\{f_b - f_{b-1}\} - j\omega a f_{b+1}\Big] \tag{42}$$

From Equation (42), we obtain:

$$aW' f_b(\bar{C}) = \Big[aW'(\bar{C}) + j\omega a - \omega^2\Big] f_{b+1} \tag{43}$$

Moreover, we obtain from Equation (43):

$$f_{b+1} = \frac{aW'(\bar{C})}{aW'(\bar{C}) + j\omega a - \omega^2} f_b \tag{44}$$

Therefore, from the recurrence Equation (44), we obtain:

$$f_b = \left[\frac{aW^{'}(\bar{C})}{aW^{'}(\bar{C}) + j\omega a - \omega^2}\right]^{b-1} f_0 \tag{45}$$

Therefore, from the stable analysis method:

$$\left|\frac{aW^{'}(\bar{C})}{aW^{'}(\bar{C}) + j\omega a - \omega^2}\right| < 1 \tag{46}$$

where, let $\omega \approx 0$. Then we obtain [12]:

$$0 < W^{'}(\bar{C}) < \frac{a}{2} \tag{47}$$

Therefore, we obtain:

$$W(t) \equiv g\left[C_b(t),\ t \geq 0\right] \tag{48}$$

where $g[\bullet]$ is determined appropriately. For example, it may be set to $g[\bullet] \in C^{\infty}$. The objective is to follow the deviation of $C(t)$ and achieve synchronization.

Assumption 6.1. *$W(\bar{C})$ has a trend coefficient μ of proportional constant.*

$$W(\bar{C}) \approx \mu\bar{C} \tag{49}$$

Thus,

$$a > 2\mu \tag{50}$$

We calculated the yield curve in Figure 12 to Figure 15 based on our actual data Testrun1-Testrun3.

With respect to a process's propagation velocity, we give the following definition.

Definition 6.1.

$$\rho_s = \frac{N}{T_c} \tag{51}$$

where $N = 6 \times 9 = 54$. N is the number of total processes and T_c is the total cycle time of the processes, ρ_s represents the average value of the process propagation velocity.

The yield in Figure 12 to Figure 15 represents a present value order of materials for production.

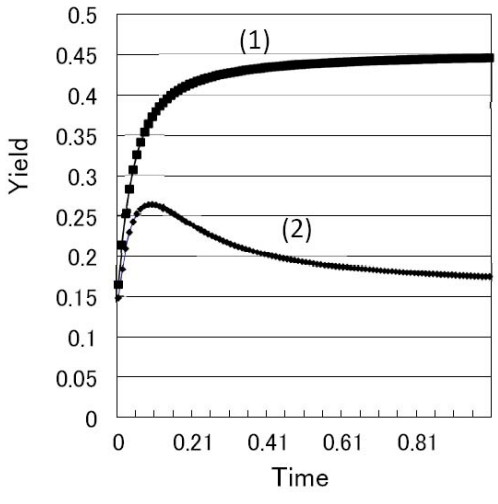

FIGURE 12. Yield of worker times

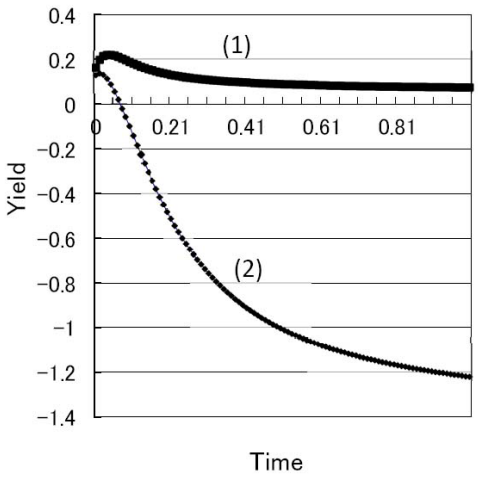

FIGURE 13. Yield of Testrun1

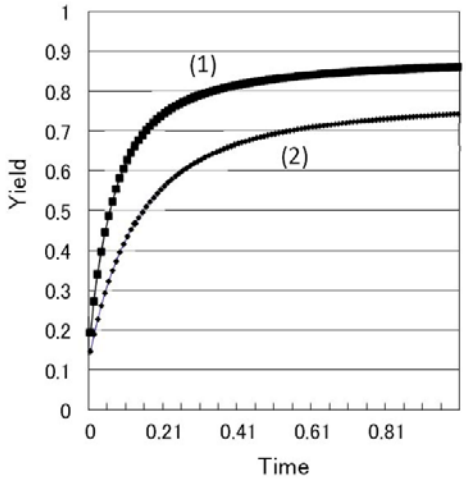

FIGURE 14. Yield of Testrun2

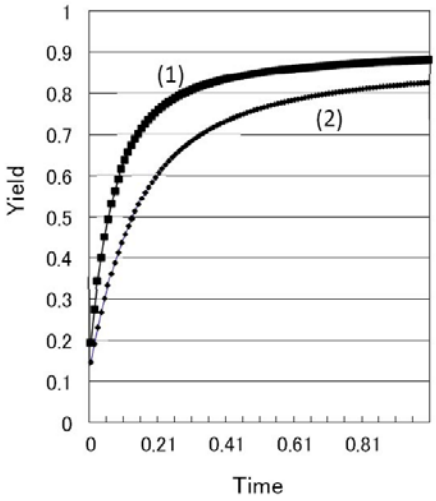

FIGURE 15. Yield of Testrun3

6.1. **Comparison based on the data collected from the three workers of Testrun1.** In Figure 12, (1) shows $a > 2\bar{\mu} = 2 \times 0.836 = 1.672$, and (2) shows $a < 2\bar{\mu} = 2 \times 0.836 = 1.672$.

A: Normalized average of the three workers

$$\bar{\mu} = \bar{\mu}_1 + \bar{\mu}_2 + \bar{\mu}_3 = \frac{0.831 + 0.948 + 0.73}{3} = 0.836$$

B: Average volatility of the three workers

$$\bar{\sigma} = \bar{\sigma}_1 + \bar{\sigma}_2 + \bar{\sigma}_3 = \frac{0.169 + 0.253 + 0.103}{3} \approx 0.175$$

C: Process propagation velocity

$$\rho_s = \frac{N}{T_c} = \frac{54}{1085 + 100(idle\ time)} \approx 0.456$$

TABLE 1. Parameter settings in Figure 12

(1)	(2)
$a_b = 0.2$	$a_c = 0.15$
$m_b = 0.836$	$m_c = 0.836$
$\sigma_b = 0.175$	$\sigma_c = 0.175$
$h_{b0} = 0.1$	$h_{b0} = 0.1$

6.2. **Comparison based on the Testrun1 data.** In Figure 13, (1) shows $a > 2\bar{\mu} = 2 \times 0.73 = 1.46$, and (2) shows $a < 2\bar{\mu} = 2 \times 0.73 = 1.46$.

A: Normalized average

$$\bar{\mu} = 0.73 \text{ (see Appendix A)}$$

B: Average volatility of three workers

$$\bar{\sigma} = 0.29 \text{ (see Appendix A)}$$

C: Process propagation velocity

$$\rho_s = \frac{N}{T_c} = \frac{54}{1085 + 100(idle\ time)} \approx 0.456$$

TABLE 2. Parameter settings in Figure 13

(1)	(2)
$a_b = 0.25$	$a_c = 0.12$
$m_b = 0.73$	$m_c = 0.73$
$\sigma_b = 0.29$	$\sigma_c = 0.25$
$h_{b0} = 0.1$	$h_{b0} = 0.1$

6.3. **Comparison based on the Testrun2 data.** In Figure 14, (1) shows $a > 2\bar{\mu} = 2 \times 0.92 = 1.84$, and (2) shows $a < 2\bar{\mu} = 2 \times 0.92 = 1.84$.

A: Normalized average

$$\bar{\mu} = 0.92 \text{ (see Appendix A)}$$

B: Average volatility of three workers

$$\bar{\sigma} = 0.06 \text{ (see Appendix A)}$$

C: Process propagation velocity

$$\rho_s = \frac{N}{T_c} = \frac{54}{1115} \approx 0.048, \text{ Ignore the idle time}$$

TABLE 3. Parameter settings in Figure 14

(1)	(2)
$a_b = 0.25$	$a_c = 0.12$
$m_b = 0.92$	$m_c = 0.92$
$\sigma_b = 0.06$	$\sigma_c = 0.06$
$h_{b0} = 0.1$	$h_{b0} = 0.1$

6.4. **Comparison based on the Testrun3 data.** In Figure 15, (1) shows $a > 2\bar{\mu} = 2 \times 0.92 = 1.84$, and (2) shows $a < 2\bar{\mu} = 2 \times 0.92 = 1.84$.

A: Normalized average

$$\bar{\mu} = 0.92 \text{ (see Appendix A)}$$

B: Average volatility of three workers

$$\bar{\sigma} \approx 0.03 \text{ (see Appendix A)}$$

C: Process propagation velocity

$$\rho_s = \frac{N}{T_c} = \frac{54}{1030} \approx 0.052, \text{ Ignore the idle time}$$

TABLE 4. Parameter settings in Figure 15

(1)	(2)
$a_b = 0.25$	$a_c = 0.12$
$m_b = 0.92$	$m_c = 0.92$
$\sigma_b = 0.03$	$\sigma_c = 0.03$
$h_{b0} = 0.1$	$h_{b0} = 0.1$

In Figures 12 and 13, $a < 2\bar{\mu}$ is clearly shown to be a more unstable state of the throughput function than $a > 2\mu$. In Figures 14 and 15, as the volatility of the total throughput is small, it is difficult to demonstrate a stable state. However, we obtain good results to satisfy the condition $a < 2\bar{\mu}$.

Then, ρ_s is an increasing function of a. Thus, there is a close relationship between the regression speed, $a(t)$, and the throughput and volatility. Therefore, as compared with Testrun2 and Testrun3, Testrun1 has many process bottlenecks scattered throughout.

In other words, the above phenomenon appears to have a phase structure consisting of a synchronous and asynchronous component. We have identified a phase transition mechanism within the phase structure.

7. **Conclusion.** In this study, we proposed an average regression model to represent a production process, and we calculated the width of a phase transition, whose exact value could not be shown in a previous study.

Moreover, we devised the representation of a stable condition. From the stable condition, we presented a calculation for maintaining stability based on actual data that were gathered by the production flow process (Appendix data). As a result, it was found that the regression speed had a close relationship with throughput and volatility. It was also found that a synchronous process had a larger throughput than an asynchronous process.

REFERENCES

[1] K. Shirai and Y. Amano, Nonlinear characteristics of the rate of return in the production process, *International Journal of Innovative Computing, Information and Control*, vol.10, no.2, pp.601-616, 2014.

[2] K. Shirai, Y. Amano and S. Omatu, Improving throughput by considering the production process, *International Journal of Innovative Computing, Information and Control*, vol.9, no.12, pp.4917-4930, 2013.

[3] K. Shirai, Y. Amano and S. Omatu, Propagation of working-time delay in production, *International Journal of Innovative Computing, Information and Control*, vol.10, no.1, pp.169-182, 2014.

[4] K. Shirai and Y. Amano, Application of an autonomous distributed system to the production process, *International Journal of Innovative Computing, Information and Control*, vol.10, no.4, pp.1247-1265, 2014.

[5] K. Shirai and Y. Amano, Production density diffusion equation propagation and production, *IEEJ Trans. Electronics, Information and Systems*, vol.132-C, no.6, pp.983-990, 2012.

[6] H. Tasaki, *Thermodynamics – From a Modern Point of View (New Physics Series)*, Baifukan Co. LTD, 2000.

[7] K. Shirai, Y. Amano, S. Omatu and E. Chikayama, Power-law distribution of rate-of-return deviation and evaluation of cash flow in a control equipment manufacturing company, *International Journal of Innovative Computing, Information and Control*, vol.9, no.3, pp.1095-1112, 2013.

[8] K. Shirai and Y. Amano, Self-similarity of fluctuations for throughput deviations within a production process, *International Journal of Innovative Computing, Information and Control*, vol.10, no.3, pp.1001-1016, 2014.

[9] K. Shirai, Y. Amano and S. Omatu, Consideration of phase transition mechanisms during production in manufacturing processes, *International Journal of Innovative Computing, Information and Control*, vol.9, no.9, pp.3611-3626, 2013.

[10] T. Nakashima, Properties of the correlation between queue length and congestion window size under self-similar, *International Journal of Innovative Computing, Information and Control*, vol.5, no.11(B), pp.4373-4381, 2009.

[11] R. Yamamoto, T. Nakaturu, K. Miyajima and M. Ishikawa, On the mathematical modeling of order-disorder transition by stochastic partial differential equations, *Yamaguchi Univ. Enjineering Faculty Reasarch Report*, vol.50, no.1, pp.45-51, 1999.

[12] Y. Sugiyama, Physics of traffic flow, *Nagare*, vol.22, pp.95-108, 2003.

[13] L. Arnold, *Random Dynamical Systems*, Springer, Berlin, 1998.

[14] C. G. Langton, Computation at the edge of chaos, *Physica D*, vol.42, 1990.

[15] K. Shirai and Y. Amano, Production throughput evaluation using the Vasicek model, *International Journal of Innovative Computing, Information and Control*, vol.11, no.1, pp.1-17, 2015.
[16] K. Kitahara, *Non-equilibrium Statistical Physics*, Iwanami Co., LTD, pp.203-214, 1997.

Appendix A. Analysis of the Testrun Results.

- (Testrun1): Because the throughput of each process (S1-S6) is asynchronous, the overall process throughput is asynchronous. In Table 6, we list the manufacturing time (min) of each process. In Table 7, we list the volatility in each process performed by the workers. Finally, Table 6 lists the target times. The theoretical throughput is obtained as $3 \times 199 + 2 \times 15 = 627$ (min). In addition, the total working time in stage S3 is 199 (min), which causes a bottleneck. In Figure 16, we plot the measurement data listed in Table 6, which represents the total working time of each worker (K1-K9). In Figure 17, we plot the data contained in Table 6, which represents the volatility of the working times.
- (Testrun2): Set to synchronously process the throughput. The target time listed in Table 8 is 500 (min), and the theoretical throughput (not including the synchronization idle time) is 400 (min). Table 9 presents the volatility of each working process (S1-S6) for each worker (K1-K9).
- (Testrun3): Introduce a preprocess stage. The process throughput is performed synchronously with the reclassification of the process. As shown in Table 10, the theoretical throughput (not including the synchronization idle time) is 400 (min). Table 11 presents the volatility of each working process (S1-S6) for each worker (K1-K9). On the basis of these results, the idle time must be set to 100 (min). Moreover, the theoretical target throughput ($T_s^{'}$) can be obtained using the "Synchronization with preprocess" method. This goal is as follows:

$$\begin{aligned} T_s &\sim 20 \times 6(\text{First cycle}) + 17 \times 6(\text{Second cycle}) \\ &\quad + 20 \times 6(\text{Third cycle}) + 20(\text{Previous process}) + 8(\text{Idol} - \text{time}) \\ &\sim 370\,(\text{min}) \end{aligned} \tag{52}$$

The full synchronous throughput in one stage (20 min) is

$$T_s^{'} = 3 \times 120 + 40 = 400\,(\text{min}) \tag{53}$$

Using the "Synchronization with preprocess" method, the throughput is reduced by approximately 10%. Therefore, we showed that our proposed "Synchronization with preprocess" method is realistic and can be applied in flow production systems. Below, we represent a description of the "Synchronization with preprocess".

In Table 10, the working times of the workers K4, K7 show shorter than others. However, the working time shows around target time. Next, we manufactured one piece of equipment in three cycles. To maintain a throughput of six units/day, the production throughput must be as follows:

$$\frac{(60 \times 8 - 28)}{3} \times \frac{1}{6} \simeq 25\,(\text{min}) \tag{54}$$

where the throughput of the preprocess is set to 20 (min). In Equation (54), the value 28 represents the throughput of the preprocess plus the idle time for synchronization. Similarly, the number of processes is 8 and the total number of processes is 9 (8 plus the preprocess). The value of 60 is obtained as 20 (min) $\times$ 3 (cycles).

In Table 5, Testrun3 indicates a best value for the throughput in the three types of theoretical working time. Testrun2 is ideal production method. However, because it is difficult for talented worker, Testrun3 is a realistic method.

TABLE 5. Correspondence between the table labels and the Testrun number

	Table number	Production process	Working time	Volatility
Testrun1	Table 6	Asynchronous process	627 (min)	0.29
Testrun2	Table 8	Synchronous process	500 (min)	0.06
Testrun3	Table 10	"Synchronization with preprocess" method	470 (min)	0.03

TABLE 6. Total manufacturing time at each stage for each worker

	WS	S1	S2	S3	S4	S5	S6
K1	15	20	20	25	20	20	20
K2	20	22	21	22	21	19	20
K3	10	20	26	25	22	22	26
K4	20	17	15	19	18	16	18
K5	15	15	20	18	16	15	15
K6	15	15	15	15	15	15	15
K7	15	20	20	30	20	21	20
K8	20	29	33	30	29	32	33
K9	15	14	14	15	14	14	14
Total	145	172	184	199	175	174	181

TABLE 7. Volatility of Table 6

K1	1.67	1.67	3.33	1.67	1.67	1.67
K2	2.33	2	2.33	2	1.33	1.67
K3	1.67	3.67	3.33	2.33	2.33	3.67
K4	0.67	0	1.33	1	0.33	1
K5	0	1.67	1	0.33	0	0
K6	0	0	0	0	0	0
K7	1.67	1.67	5	1.67	2	1.67
K8	4.67	6	5	4.67	5.67	6
K9	0.33	0.33	0	0.33	0.33	0.33

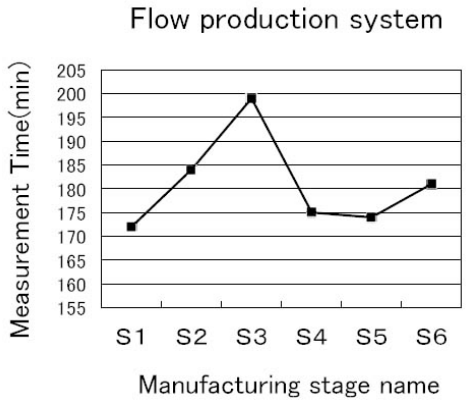

FIGURE 16. Total work time for each stage (S1-S6) in Table 6

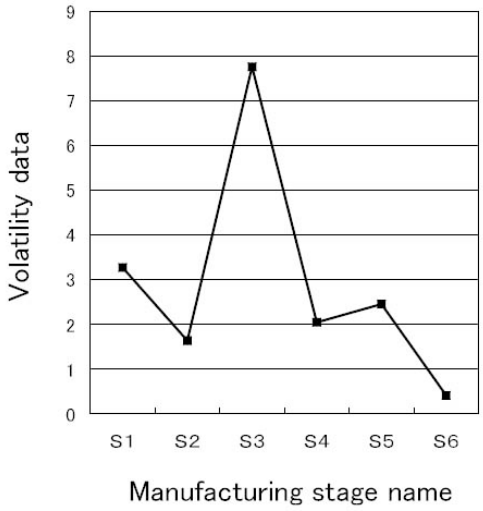

FIGURE 17. Volatility data for each stage (S1-S6) in Table 6

The results are as follows. Here, the trend coefficient, which is the actual number of pieces of equipment/the target number of equipment, represents a factor that indicates the degree of the number of pieces of manufacturing equipment.
Testrun1: 4.4 (pieces of equipment)/6 (pieces of equipment) = 0.73,
Testrun2: 5.5 (pieces of equipment)/6 (pieces of equipment) = 0.92,
Testrun3: 5.7 (pieces of equipment)/6 (pieces of equipment) = 0.95.
Volatility data represent the average value of each Testrun.

TABLE 8. Total manufacturing time at each stage for each worker

	WS	S1	S2	S3	S4	S5	S6
K1	20	20	24	20	20	20	20
K2	20	20	20	20	20	22	20
K3	20	20	20	20	20	20	20
K4	20	25	25	20	20	20	20
K5	20	20	20	20	20	20	20
K6	20	20	20	20	20	20	20
K7	20	20	20	20	20	20	20
K8	20	27	27	22	23	20	20
K9	20	20	20	20	20	20	20
Total	180	192	196	182	183	182	180

TABLE 9. Volatility of Table 8

K1	0	1.33	0	0	0	0
K2	0	0	0	0	0.67	0
K3	0	0	0	0	0	0
K4	1.67	1.67	0	0	0	0
K5	0	0	0	0	0	0
K6	0	0	0	0	0	0
K7	0	0	0	0	0	0
K8	2.33	2.33	0.67	1	0	0
K9	0	0	0	0	0	0

TABLE 10. Total manufacturing time at each stage for each worker, K5 (*): Preprocess

	WS	S1	S2	S3	S4	S5	S6
K1	20	18	19	18	18	18	18
K2	20	18	18	18	18	18	18
K3	20	21	21	21	21	21	21
K4	16	13	11	11	13	13	13
K5	16	*	*	*	*	*	*
K6	16	18	18	18	18	18	18
K7	16	14	14	13	14	14	13
K8	20	22	22	22	22	22	22
K9	20	20	20	20	20	20	20
Total	148	144	143	141	144	144	143

TABLE 11. Volatility of Table 10, K5 (*): Preprocess

K1	0.67	0.33	0.67	0.67	0.67	0.67
K2	0.67	0.67	0.67	0.67	0.67	0.67
K3	0.33	0.33	0.33	0.33	0.33	0.33
K4	1	1.67	1.67	1	1	1
K5	*	*	*	*	*	*
K6	0.67	0.67	0.67	0.67	0.67	0.67
K7	0.67	0.67	1	0.67	0.67	1
K8	0.67	0.67	0.67	0.67	0.67	0.67
K9	0	0	0	0	0	0